A COMPARISON OF METHOD FOR ESTIMATING FRACTIONAL GREEN VEGETATION COVER DERIVED FROM HYEPRION HYPERSPECTRAL DATA

Yeosang Yoon and Yongseung Kim

Remote Sensing Department, Korea Aerospace Research Institute
45 Eoeun-Dong, Youseong-Gu, Daejeon 305-333, Korea
Tel: (82)-42-860-2276 Fax: (82)-42-860-2605
E-mail: gise@kari.re.kr, yskim@kari.re.kr

ABSTRACT: Green vegetation is one of the most critical factors for environment conditions thorough modulating evapotranspiration and absorption of solar radiation. Thus, fractional green vegetation cover (FVC) plays an important role in observing and managing environment. Remote sensing provides a seemingly obvious data source for quantifying FVC over large area. Therefore we compared a set of methods for estimating FVC using hyperspectral remote sensing data. For our study, we used Hyperion imagery acquired in April, 2002. In order to achieve our efforts, we analyzed simple NDVI-based method and spectral mixture analysis (SMA) models that were applied a variety of combinations of possible endmembers.

KEY WORDS: fractional green vegetation, NDVI, spectral mixture analysis, Hyperion

1. INTRODUCTION

Green vegetation is one of the most important roles in the exchange of carbon, water, and energy at the land surface (Tueller, 1987; Xiao and Moody, 2005). Thus, fractional green vegetation cover (FVC) plays an important role in observing and managing environment (Gutman and Ignatov, 1998). In addition, FVC is also a sensitive indicator of land degradation and desertification in arid and semi-arid regions. Remote sensing provides a seemingly obvious data source for quantifying FVC over large area.

Vegetation is often sparsely distributed and the area contain spectral that the mixed reflectance of green vegetation (GV), non-photosynthetic vegetation (NPV), bare soil, and shadow. Thus, units of vegetation are not individually resolved. Spectral mixture model (SMA) has often been used to estimate subpixel canopy proportions from multispectral or hyperspectral satellite data (Dennison *et al.*, 1999; Roberts *et al.*, 2003).

In this study, we compared two-endmember SMA, three-endmember SMA, four-endmember SMA, and the NDVI for estimating FVC in heterogeneous region from Hyperion, an imaging spectrometer on the Earth Observation 1 (EO-1) satellite platform. For our study, we derived endmember spectra from Hyperion image including GV, NPV, bare soil, and shadow. The results of FVC were validated by comparing the true color high resolution orthoimagery.

2. BACKGROUND

It is commonly noted that reflectance spectra derived from satellite-based sensors constitute mixed signals, in particular when the sizes of scene objects are smaller than the instantaneous field of view (Jensen, 1996). The most common approach for characterizing ground cover at the sub-pixel scale using remote sensing data is SMA (Smith *et al.*, 1990; Tompkins *et al.*, 1997; Roberts *et al.*, 2003) although other methods have also been used including artificial neural networks, fuzzy classifiers, maximum likelihood classifiers, regression trees, decision trees, and simple regression based on NDVI (Elmore *et al.*, 2000).

SMA technique assumes that the remotely sensed surface reflectance can be modeled as the linear combination of endmember reflectance spectra (Smith *et al.*, 1990). Endmember spectra (i.e., laboratory, reference, or image pixel spectra) are selected to represent the physical scene components of interest, but they also must adequately explain the majority of scene spectral variance. SMA proceeds with the formation of the following system of equations for each pixel in the image:

$$R_{mix,b} = \sum (f_{em} R_{em,b}) + \varepsilon_b \quad and \quad \sum f_{em} = 1 \qquad (1)$$

where $R_{mix,b}$ is reflectance of observed image spectrum at each band; f_{em} is fraction of each endmember in

observed mixed spectrum; $R_{em,b}$ is reflectance of each endmember at each band; ε_b is band residual.

3. METHOD

3.1 Study Site

The study site is located in southwest part of GyeongGi-Do, Korea. This area consists of forest, farmland and small village. Although many species of trees are present, only a few species dominate the landscape including pine and oak.

3.2 Data

For our study, we used part of the Hyperion imagery acquired at approximately 02:00 UTC on April 3, 2002. Hyperion is a hyperspectral instrument on the Earth Observing 1 (EO-1) spacecraft that was launched on November 21, 2000. Hyperion imagery consists of 242 channels ranging from 356-2577nm, sampled approximately at a 10nm sampling interval. It is part of EO-1 platform and follows Landsat Enhanced Thematic Mapper (ETM) in its orbits, providing nearly simultaneous coverage. Each image contains data for a 7.65km wide (cross-track) by 185km long (along-track) region.

3.3 Image Analysis

3.3.1 Detection and Correction of Abnormal Pixels: Hyperion acquires data in pushbroom mode with two spectrometers, one in the visible and near infrared (VNIR) range and another in the short-wave infrared (SWIR) range. We used Hyperion data set is called hyperion level 1b, which is radiometrically-corrected all bad pixels. However, bad pixels are still evident. In addition, there are dark vertical stripes in the image (Han *et al.*, 2002). In order to correct the abnormal pixels, we applied modified 3×3 average Filter to atypical pixels.

3.3.2 Atmospheric correction: The Hyperion data was radiometrically corrected to reflectance using the FLAASH (Fast Line of sight Atmospheric Analysis of Hyperspectral Cubes) ver. 4.2. The surface reflectance was determined by the following equation:

$$L = \left(\frac{A\rho}{1-\rho_e S}\right) + \left(\frac{B\rho_e}{1-\rho_e S}\right) + L_a \qquad (2)$$

where ρ is the pixel surface reflectance; ρ_e is an average surface reflectance for the pixel; S is the spherical albedo of the atmosphere; L_a is the radiance back scattered by the atmosphere; A and B are coefficients that depend on atmospheric and geometric condition but not on the surface.

3.3.3 NDVI method: The traditional broadband vegetation indices (VIs), such as Thematic Mapper (TM)-derived normalized difference vegetation index (NDVI), have been widely applied to estimate canopy. The broadband indices, usually constructed with near-infrared (NIR) and red (R) bands, use average spectral information over broad bandwidths, resulting in loss of critical information available in specific narrow bands. In addition, the broadband indices are known to be heavily affected by soil background at low vegetation cover. Thus, in this study, according to Gong *et al.*'s study, we used SWIR instead of NIR bands

$$NDVI = \frac{(\rho_{823} - \rho_{1648})}{(\rho_{823} + \rho_{1648})} \qquad (3)$$

3.3.4 SMA model: For SMA2, SMA3, and SMA4, we derived endmember spectra from the Hyperion image. Four endmembers were selected including green vegetation (GV), non-photosynthetic vegetation (NPV), bare soil, and shadow. The endmembers were selected from pure pixels with reference to the field spectrometer (GER3700) and high resolution orthoimagery

With a total four endmembers considered and GV and NPV endmember always used, there were 1 possible two-endmember combination for SMA2 model, 2 possible three-endmember combinations for SMA3 models, and 1 possible four-endmember for SMA4 model. For each model, all endmember models were selected from the library of potential models based on whether they are physically reasonable (fraction are between 0% and 100%) and meet criteria based on the overall fit and residuals.

3.3.5 Validation: The results of NDVI and SMA were validated by comparing the true-color high resolution orthoimagery (1m resolution). We randomly selected 13 pixels from the Hyperion image, and the orthoimagery was used to estimate the actual fraction within 3×3 window around each sampled Hyperion pixel (Actually, we used 117 pixels from Hyperion image). Thus, for each sample (i.e., 3×3 window at Hyperion resolution), actual fraction was estimated from a corresponding 90×90 pixels subset from the 3-band, true-color orthoimagery. Each orthoimagery subset was classified, using maximum likelihood classification, into GV, NPV, shadow, and soil. Each orthoimagery subset was separately classified based on training data selected from the subset.

4. RESULTS/DISCUSSION

4.1 Detection and Correction of Abnormal pixels

There are many possible causes for the abnormal pixels including detector failure, errors during data transfer, and improper data correction. We corrected the abnormal pixels and removed atypical bands. Finally, we used 150 bands of 242 bands.

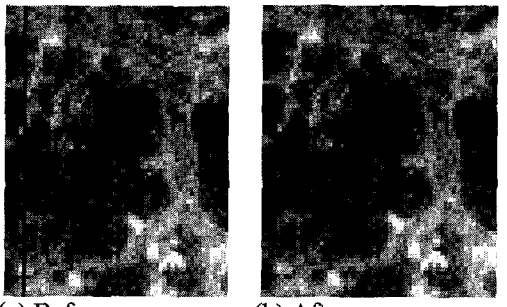

(a) Before (b) After

Figure 1. Abnormal pixel correction

4.2 NDVI

NDVI was constructed from the SWIR (1648nm) and NIR (823nm) regions instead of NIR and R bands. These bands are related to plant leaf water content that has a close correlation with canopy biomass and indirectly to the absorption features of protein, nitrogen, lignin, cellulose and starch concentrations.

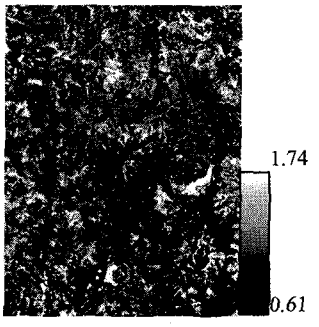

Figure 2. Image showing NDVI for Hyperion imagery

4.3 SMA

Hyperion results exhibited recognizable pattern of GV, NPV, shadow and Soil (Figure 3). On the whole, each of SMA result showed similar pattern. In this figure, areas mapped as a green (GV) are considered the presence of large amounts of live leaf material with its associated moisture. Areas with high NPV fractions are considered to have high fire danger because of an abundance of senesced plant material.

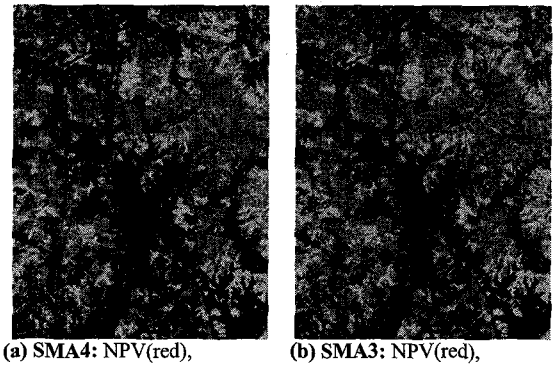

(a) SMA4: NPV(red), GV(green), and shadow(blue)

(b) SMA3: NPV(red), GV(green), and shadow(blue)

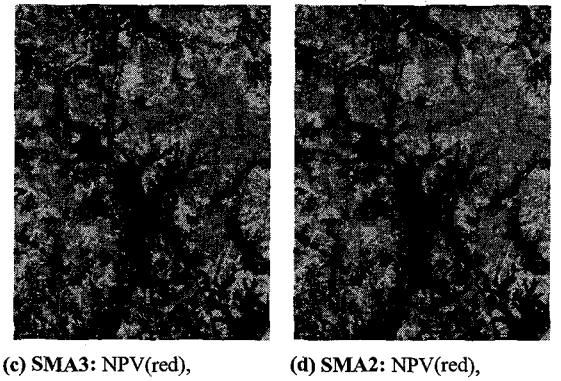

(c) SMA3: NPV(red), GV(green), and soil(blue)

(d) SMA2: NPV(red), GV(green), and NPV(blue)

Figure 3. False color composite showing fraction images

4.4 Validation

The accuracy of SMA and NDVI results was compared using high resolution orthoimagery (Figure 4).

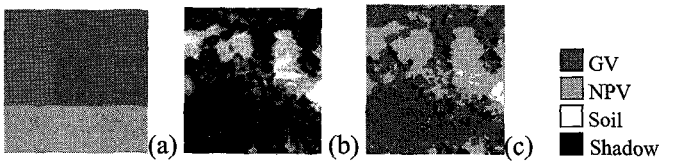

Figure 4. The estimation of actual fraction within 3×3 window surrounding each sample Hyperion pixel from high resolution orthoimagery. (a) is the SMA result subset with NPV(red), GV(green), and Soil(blue); (b) is orthoimagery; (c) is classified image of the orthoimagery subset.

The overall performance of SMA model and NDVI provided good result and matched well (nearly linear) actual fractional green vegetation cover derived high resolution orthoimagery (Figure 5 and Table 1). In addition, the simple method for estimating fractional green vegetation cover from NDVI showed relatively good performance.

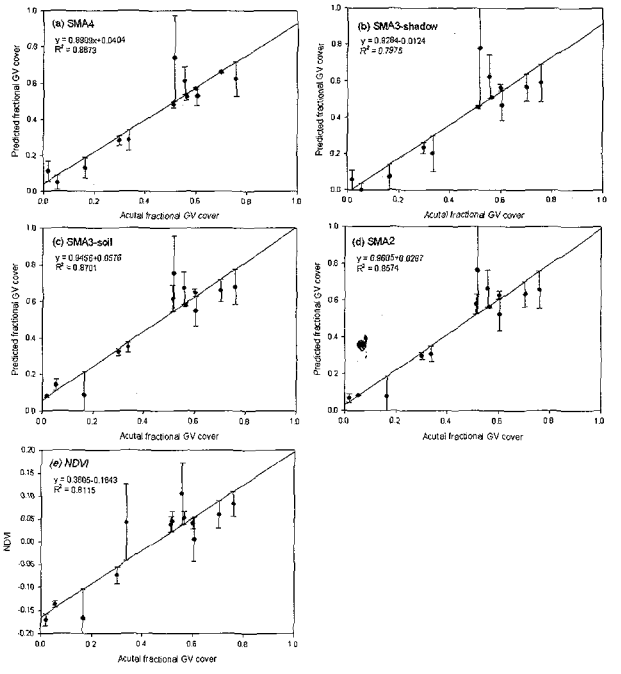

Figure 5. Relationship between actual and predicted fractional green vegetation cover (FVC)

Table 1. R^2 and RMSE values between actual vegetation fraction and vegetation fraction predicted from each method

	SMA4	SMA3 (shadow)	SMA3 (soil)	SMA2	NDVI
R^2	0.87	0.80	0.87	0.86	0.82
RMSE	0.085	0.118	0.092	0.092	-

5. CONCLUSION

In this study, we used spectral mixture analysis and NDVI to estimate the fractional green vegetation cover using hyperspectral image.

Hyperion image had many possible errors for the abnormal pixels including detector failure, errors during data transfer, and improper data correction. First of all, we eliminated those error pixels and atypical bands. Atmospheric correction was also corrected using FLAASH module. NDVI for estimating fractional green vegetation was very simple, but the result showed considerably good compared with others method. Spectral mixture analysis showed a powerful, multifaceted tool for this approach. However, the accuracy of SMA depends on the accuracy of endmember selection. Thus, the selection of endmember plays an important role in this processing. Our results suggest that three or four endmembers may be adequate to estimate the fractional vegetation cover, but we need further repetitive studies for improving the representation of the spectral variability of land-cover types.

REFERENCES

References from Journals:

Gutman, G., and Ignatov, A., 1998. The derivation of the green vegetation fraction from NOAA/AVHRR data for use in numerical weather prediction models. *International Journal of Remote Sensing*, 19, pp.1533-1543

Dennision, P. E., Robers, D. A., and Regelbrugge, J. C., 2000. Characterizing chaparral fuels using combined hyperspectral and synthetic aperture radar data. *In Proc. 9th AVIRIS Earth Science Workshop*, 6, pp. 119-124

Elmore, A. J., Mustard J. F., Manning, S. J., and Lobell, D. B., 2000, Quantifying vegetation change in semiarid environments: Precision and accuracy of spectral mixture analysis and the normalized difference vegetation index. *Remote Sensing of Environment*, 73, pp. 87-102

Han, T., Goodenough D. G., Dyk, A., and Love, L., 2002, Detection and correction of abnormal pixels in hyperion images, ?

Roberts, D. A., Dennison, P. E., Gardner, M. E., Hetzel, Y., Ustin, S. L., and Lee C. T., 2003. Evaluation of the potential of hyperion for fire danger assessment by comparison to the airborne visible/infrared imagine spectrometer. *IEEE Trans. Geoscience Remote Sensing*, 41(6), PP.1297-1310

Smith, M. O., Ustin, S. L., Adams, J. B. and Gillespie, A. R., 1990. Vegetation in deserts: I. A regional measure of abundance from multispectral images. *Remote Sensing of Environment*, 31, pp. 1-26

Tueller, P.T., 1987. Remote sensing science applications in arid environments. *Remote Sensing of Environment*, 23, pp. 143-154

Tompkins, S., Mustard, J. F., Pieters, C. M., and Forsyth D. W., Optimization of endmembers for spectral mixture analysis. . *Remote Sensing of Environment*, 59, pp. 472-489

Xiao, J. and Moody, A., 2005. A comparison of methods for estimating fractional green vegetation cover within a desert-to-upland transition zone in central New Mexico, USA, . *Remote Sensing of Environment*, 98, pp. 237-250

References from Books:

Jensen, J. R., 1996. *Introductory digital image processing: A remote sensing perspective*. Prentice Hall, second edition.